How Carbon Monoxide Adsorbs in Different Sites

A. Föhlisch,[1] M. Nyberg,[2] J. Hasselström,[1] O. Karis,[1] L. G. M. Pettersson,[2] and A. Nilsson[1]

[1]*Department of Physics, Uppsala University, Box 530, S-751 21 Uppsala, Sweden*

[2]*FYSIKUM, University of Stockholm, Box 6730, S-113 85 Stockholm, Sweden*

(Received 11 October 1999)

The interplay between the electronic and the geometric structure of adsorbates is of fundamental importance for the understanding of many surface phenomena. Using x-ray emission spectroscopy and *ab initio* cluster calculations, this issue has been investigated in unprecedented detail for CO adsorption in different adsorption sites. The investigation establishes π bonding and σ repulsion, both increasing with the number of coordinated metal atoms. The two contributions partly compensate each other, leading to only small differences in adsorption energies for the different adsorption sites despite very large variations in the electronic structure.

PACS numbers: 82.65.My, 73.20.Hb, 78.70.En, 82.20.Wt

Over the years there has been an enormous experimental and theoretical effort to develop a detailed atomic picture of chemical interactions at surfaces which are important in many different fields such as heterogeneous catalysis, corrosion, electrochemistry, and molecular environmental science [1]. Most often, the focus has been to identify the chemical state and geometric structure of adsorbed molecules. However, if we want to have a chemically intuitive picture we need to understand why the atoms are located in a specific way and why certain species are more reactive. The answer is directly related to the electronic structure and to the nature of the chemical bond.

In this Letter, we address the interplay between the electronic and the geometric structure systematically on a fundamental level by studying the prototypical system of CO adsorbed in different positions on a metal surface. Molecular CO is known for its ability to populate different adsorption sites, depending on the metal, substrate structure, coverage, temperature, and influence from coadsorbate species [2]. Here, CO adsorbed in on-top, bridge, and hollow sites on Ni(100) and H/Ni(100) has been considered [3,4]. These often coexisting phases indicate only small energetic differences for different sites, which has been interpreted as an indication of rather similar bonding. At the same time, it is known from vibrational spectroscopy that the CO intramolecular bond is affected differently in the different sites [3]. The CO stretch frequency decreases with increasing coordination to the metal substrate [5]. The weakening of the internal CO bond, as evident through the frequency shift, has in the past been discussed in terms of backdonation of substrate electrons into the previously unoccupied antibonding CO $2\pi^*$ orbital [6–10]. The degree of backdonation was thought to increase with increasing coordination of the CO to the metal atoms [5,11,12].

In order to directly probe the orbitals involved in the surface chemical bond we need a method that allows us not only to separate out orbitals on the adsorbed entity, but also to spotlight one atom at a time, i.e., an atom-specific probe. x-ray emission spectroscopy (XES) applied to adsorbates has in recent years been shown to be a spectroscopy well suited for obtaining atom-specific and symmetry selective electronic structure information due to the localization of the core intermediate state [13–16]. This allows one to divide the total density of electronic states into atom and symmetry selected partial densities of states, which furthermore provides a very strong basis for the evaluation of theoretical methods for molecular orbital population analysis [17].

We will in this paper show that the adsorption of CO on a metal such as Ni involves a balance of π bonding and σ repulsion. Both the σ and π electronic structures result from strong orbital mixing within each symmetry group. The π bonding is manifested through the creation of new orbitals unique for the adsorbate complex, where in particular one of them is of O lone pair character. In order to develop the new orbitals we need to involve both the occupied 1π and unoccupied $2\pi^*$ orbitals of the CO molecule resulting in a net bonding configuration. The mixing of bonding and antibonding CO orbitals causes a weakening of the intramolecular bond, explaining the reduction of the C-O stretch frequency. Both the π bonding and σ repulsion increase with the number of Ni atoms directly coordinated to the CO molecule. The two contributions partly compensate each other causing a relatively small difference in adsorption energy between the different sites.

The experiments were performed on beam line 8.0 at the ALS with a bandwidth of 0.2 eV for C1s and 0.8 eV for O1s. The XE spectrometer [18] was operated at 0.5 eV resolution. The direction of detection is variable which allows a separation of XE originating from states of π and σ symmetry [14]. The on-top species was generated as the $c(2 \times 2)$ overlayer on pure Ni(100), the bridge and hollow species in coadsorption with H [4]. In the bridge site, due to relative low hydrogen coverage, the local bonding properties are not much affected by the hydrogen [3,4,19]. However, the hollow site can be populated only in the presence of hydrogen and can therefore be significantly affected. Resonant excitation into the adsorbate $2\pi^*$ orbital was performed [14,16]. Computationally,

density functional theory (DFT) [20] using gradient corrected functionals has been applied, as implemented in the deMon code [21]. An all-electron cluster representation of the adsorption system has been used: for on-top and hollow species, a Ni_{13} cluster, and for the bridge species a Ni_{14} cluster. All calculations were carried out representing a clean Ni surface with one CO molecule.

Let us begin with the XE spectra for CO in different sites, as shown in Fig. 1. The carbon and oxygen XE spectra share a common binding energy scale relative to the Fermi level by subtracting the respective core level binding energies [17,22]. On the left side of Fig. 1, states of π symmetry are displayed and on the right side states of σ symmetry. All spectral features with a binding energy above 5 eV can be readily assigned in accordance with previous photoemission measurements [4]. Theoretical spectra have been generated with good agreement to experiment [16]. Furthermore, the transition probabilities of the 1π have been used to normalize the carbon and oxygen XE relative intensities. From these calculations, orbital contour plots have also been generated of the most interesting valence orbitals in CO gas and adsorbed on a Ni_{13} cluster in on-top and hollow sites, as shown in Figs. 2 and 3 for π and σ symmetry, respectively. On the basis of these, the adsorbate orbitals can be discussed in a conceptually simple way in terms of their molecular or metallic character.

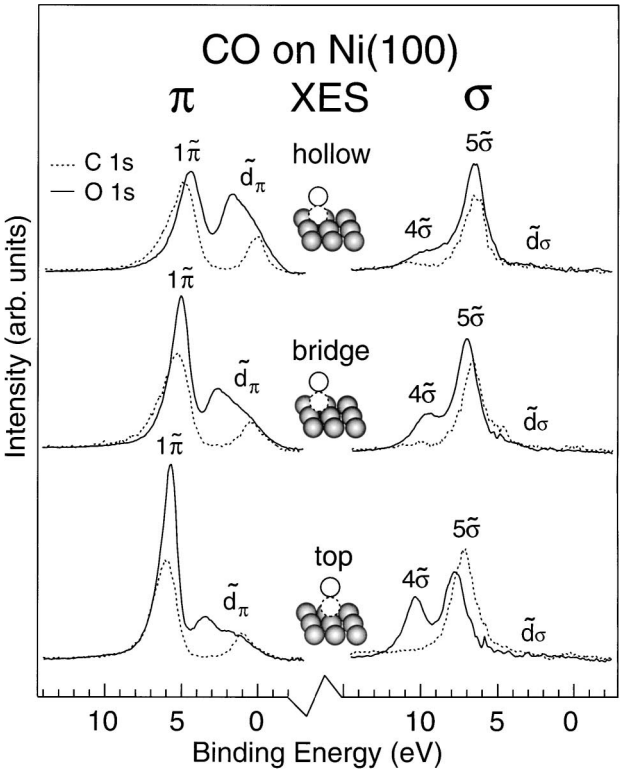

FIG. 1. Carbon and oxygen K-edge x-ray emission spectra of CO adsorbed on Ni(100) in on-top, bridge and hollow sites. The energy scale is relative to the Fermi level.

We will start by considering the general characteristics of CO surface bonding from the experimental and theoretical results. Both the π- and σ-electronic structures of the adsorbate result from a hybridization of the initial CO orbitals with the metal states, leading to a significant modification of the orbital structure in comparison to free CO. It is through the molecular π system that the bonding interaction with the surface takes place [16]. A polarization of the 1π orbital towards the carbon site is found and new states ($\tilde{d}_\pi$) appear in the energy region between 5 eV and the Fermi level. Both the polarization and intensity of the new states increase with increasing Ni coordination. In the two middle panels of Fig. 2, orbital contour plots from two different energy regions within the $\tilde{d}_\pi$ band are shown. We have labeled the orbital representing the high-energy region at the "bottom of the band" as the $\tilde{d}_\pi$-b and the orbital close to the Fermi-level at the "top of the band" as $\tilde{d}_\pi$-t. The new states are mainly of oxygen lone pair character with some carbon contribution close to the Fermi level ($\tilde{d}_\pi$-t). In the hollow site, the O lone pair intensity in the XE spectrum has even become similar to the O 1π intensity. This is somewhat surprising since a simple $2\pi^*$ backdonation picture should give an occupied $2\pi^*$-Ni $3d$ hybrid orbital with a molecular contribution similar to

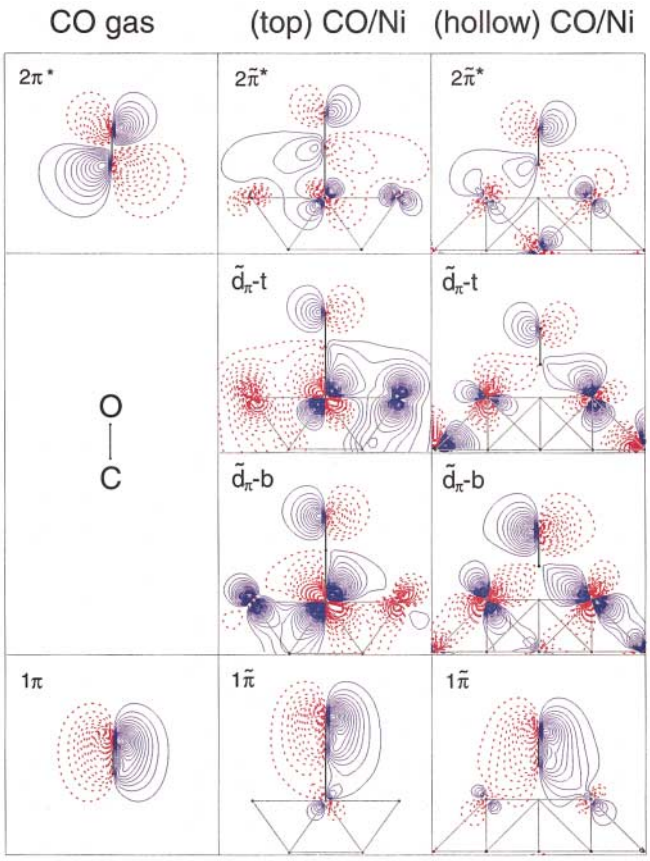

FIG. 2 (color). Contour plots of π orbitals for CO in the gas phase and adsorbed on Ni(100) in on-top and hollow sites. Line spacing in panels: (top) 0.02, (center) 0.01, (bottom) 0.02. Solid and dashed lines indicate change of phase.

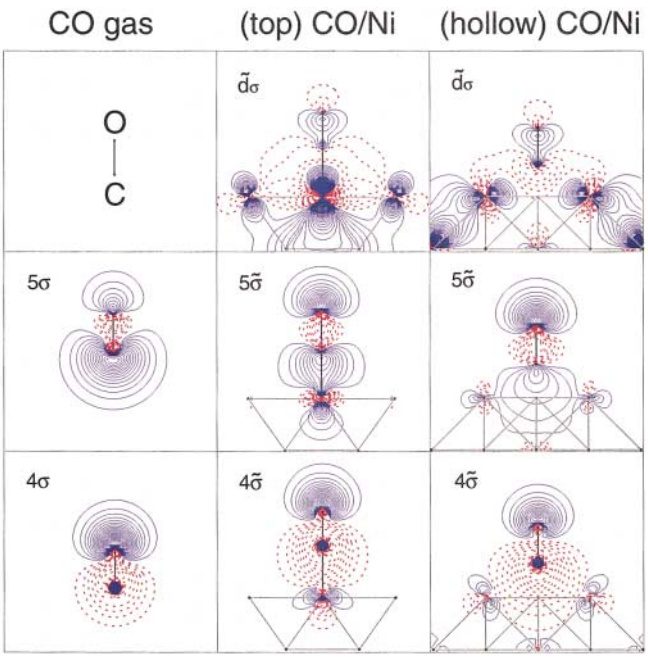

FIG. 3 (color). Contour plots of σ orbitals for CO in the gas phase and adsorbed on Ni(100) in on-top and hollow sites. Line spacing in panels: (top) 0.01, (center and bottom) 0.02. Solid and dashed lines indicate change of phase.

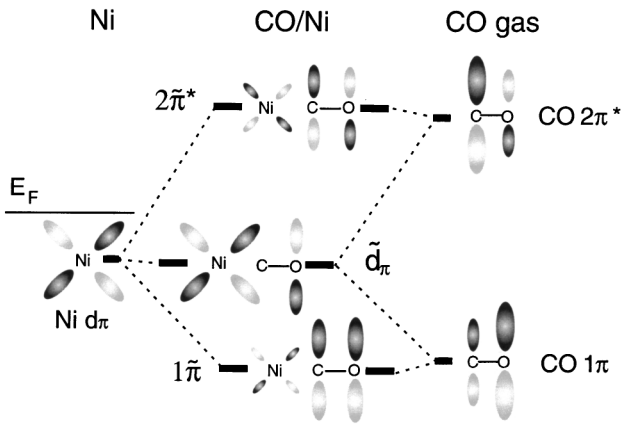

FIG. 4. Schematic orbital diagram of the π-orbital structure. An allylic configuration is formed in the model of a single CO molecule interacting with a Ni atom.

the gas phase $2\pi^*$ virtual orbital which is located mainly on the carbon atom. How can we understand that the interaction generates an essentially nonbonding O lone pair orbital?

Figure 4 summarizes, in a schematic molecular orbital picture, the π interaction between the CO and the metal. For simplicity let us consider only a single CO molecule interacting with one Ni atom, representing on-top adsorption. Three atoms are involved, and consequently three hybrid π orbitals are generated in an allylic configuration [16,17,23]. The lowest orbital is bonding among all atomic centers and the highest orbital is antibonding. The intermediate orbital has one nodal plane and has in many cases no contribution to the middle carbon atom, which makes it nonbonding. The bonding orbital $1\tilde{\pi}$ is similar to the free molecule 1π orbital with a small but significant contribution from the Ni $3d$ orbital. The intermediate orbital is nonbonding with a main contribution from the metal and can be directly assigned to the O lone pair state seen in Figs. 1 and 2. The antibonding orbital $2\tilde{\pi}^*$ is unoccupied and the molecular character is similar to the $2\pi^*$ orbital of the free molecule with major contributions from the Ni $3d$ and $4p$ orbitals and has been observed in the x-ray absorption (XA) spectra of CO in different sites on Ni(100) [19]. As the antibonding $2\tilde{\pi}^*$ remains unoccupied, the π interaction is attractive.

An important question is how the molecular orbitals of the free CO molecule are transformed into the new electronic structure of the adsorbate complex. As indicated in Fig. 4, the O lone pair orbital in the $\tilde{d}_\pi$ band is formed in first-order perturbation by an antibonding 1π and a bonding $2\pi^*$ admixture to the Ni $3d$ band. This leads to a cancellation of orbital amplitude at the carbon atom and enforcement at the oxygen atom [23]. The $1\tilde{\pi}$ is formed by a bonding admixture of the Ni $3d$ to the CO 1π and internal mixing with the CO $2\tilde{\pi}^*$, which leads to a polarization towards the metal. The π interaction is site dependent and increases with increasing coordination to the Ni substrate, which is manifested in the increasing $1\tilde{\pi}$ polarization and the increasing $\tilde{d}_\pi$-band intensity in Figs. 1 and 2.

The bonding to the metal substrate is accompanied by a weakening of the internal C-O bond through the mixing of the CO 1π and $2\pi^*$ orbitals. In a valence bond concept, we can see this as a partial breaking of the internal CO π bond, partially compensated by the surface bond. This increases the C-O bond length and decreases the internal CO stretch frequency.

The XE spectra in Fig. 1 and the orbital contour plots in Fig. 3 show strong variations also in the σ system for CO adsorbed in different sites. In the free molecule the 5σ orbital is strongly polarized to the carbon atom and the 4σ to the oxygen atom. Upon adsorption we observe a dramatic redistribution of the two σ molecular orbitals. The 5σ orbital moves towards the oxygen atom and the 4σ towards the carbon (mainly as C$2s$), and we also find a net loss of C$2s$ character in the σ symmetry. This is in line with a recent XES study of CO [16] and the isoelectronic N_2 on Ni(100) which showed a similar σ redistribution [14,17]. Figures 1 and 3 directly show how the degree of polarization increases with increasing Ni coordination, i.e., from on-top to bridge to hollow adsorption sites.

The σ system can be summarized in a molecular orbital diagram, similar to the allylic configuration of the π system. However, for symmetry reasons more orbitals are involved (C$2s$, C$2p$, O$2s$, O$2p$, and the Ni bands), making the situation more complicated. We can depict some of the highest orbitals as the $4\tilde{\sigma}$ and $5\tilde{\sigma}$ with mainly adsorbate character and the $\tilde{d}_\sigma$ orbitals with mainly metal character (see Fig. 3). The $4\tilde{\sigma}$ and $5\tilde{\sigma}$ are bonding orbitals and

undergo a shift to larger binding energy in comparison to the free molecule, whereas the metal $\tilde{d}_\sigma$ orbitals are antibonding and shift towards lower binding energies [24]. In total, the σ interaction is repulsive, since no low-lying unoccupied σ^* orbitals exist on the CO unit to allow an easy polarization of the 4σ and 5σ orbitals. The CO σ^* orbital has been observed 20 eV above the $2\pi^*$ in XAS. This large energetic separation makes the orbital mixing energetically very costly, which is the essential difference compared to the π system, where the orbital mixing involved low-lying unoccupied orbitals. The polarization within the CO σ system can be interpreted as due to a Pauli repulsion between the CO σ system and the Ni states [16,17,25]. In order to minimize this repulsion there is also a polarization of the $4sp$ density from the central Ni atom towards the surrounding metal centers. It is interesting to note that this picture is rather different compared with the often considered 5σ donation bonding scheme [5,9]. An estimate of the repulsive σ interaction is obtained by calculating the initial repulsion between the unperturbed CO molecule and the substrate brought into the equilibrium bonding distance. The computed Pauli repulsion in this case is 3.3, 5.6, and 10.3 eV for on-top, bridge and hollow sites, respectively. It directly scales with the amount of σ polarization seen experimentally (as shown in Fig. 1).

We can now understand the reason for the rich chemistry, with many different possible adsorption sites, of CO adsorbed on metals. The energetics of π bonding and σ repulsion partly compensate each other. Both increase with increasing Ni coordination in such a way that the adsorption energy is rather similar between on-top and bridge sites and slightly unfavorable for hollow sites. However, the interaction is very different between the sites, causing a dramatic change in the electronic structure which increases with increasing Ni coordination. Based on these findings, we can understand the change in vibrational frequencies and different reactivity for CO in the different adsorption sites. In adsorption systems where the π interaction is weaker, such as CO on Cu or N_2 on Ni(100), the σ repulsion will become too dominant at higher coordination, leading to population of only on-top sites.

In summary, we have shown an example of how the geometric and electronic structure of a molecular adsorbate, i.e., CO, is the result of a balance between the σ and π interactions; both in terms of total energy and local bond properties. To obtain these results, x-ray emission spectroscopy in combination with *ab initio* calculations was instrumental. Strong orbital mixing within each orbital symmetry is found: the π interaction is attractive and weakens the internal CO bond while the σ interaction is repulsive. Both the π and σ interactions increase with higher coordination. In consequence, the electronic structure for CO in the different adsorption sites varies strongly, although the adsorption energy varies comparatively little, due to the compensation between the π and σ interactions.

This work was supported by the Swedish Natural Science Research Council (NFR) and by the Göran Gustafsson Foundation for Research in Natural Sciences and Medicine. The ALS is supported by the U.S. Department of Energy. Valuable support by N. Mårtensson, J. Nordgren, and J. Stöhr is gratefully acknowledged.

[1] G. A. Somorjai, *Introduction to Surface Chemistry and Catalysis* (Wiley, New York, 1994).
[2] *The Chemical Physics of Solid Surfaces and Heterogeneous Catalysis,* edited by D. A. King and D. P. Woodruff (Elsevier, Amsterdam, 1990), Vol. 3.
[3] L. Westerlund, L. Jönsson, and S. Andersson, Surf. Sci. **199**, 109 (1988).
[4] H. Tillborg, A. Nilsson, and N. Mårtensson, Surf. Sci. **273**, 47 (1992).
[5] G. Blyholder, J. Phys. Chem. **68**, 2772 (1964).
[6] S.-S. Sung and R. Hoffmann, J. Am. Chem. Soc. **107**, 578 (1985).
[7] E. Wimmer *et al.,* Phys. Rev. Lett. **55**, 2618 (1985).
[8] G. te Velde and E. Baerends, Chem. Phys. **177**, 399 (1993).
[9] B. Hammer, Y. Morikawa, and J. K. Nørskov, Phys. Rev. Lett. **76**, 2141 (1996).
[10] F. Delbecq, Surf. Sci. **389**, 1131 (1997).
[11] K.-M. Schindler *et al.,* J. Electron Spectrosc. Relat. Phenom. **64–65**, 75 (1993).
[12] M. E. Davila *et al.,* Surf. Sci. **311**, 337 (1994).
[13] A. Nilsson *et al.,* Phys. Rev. B **51**, 10 244 (1995).
[14] A. Nilsson, M. Weinelt, T. Wiell, P. Bennich, O. Karis, N. Wassdahl, J. Stöhr, and M. G. Samant, Phys. Rev. Lett. **78**, 2847 (1997).
[15] A. Föhlisch, J. Hasselström, P. Bennich, N. Wassdahl, O. Karis, A. Nilsson, L. Triguero, M. Nyberg, and L. G. M. Pettersson, Phys. Rev. B **61**, 16 229 (2000).
[16] A. Föhlisch, M. Nyberg, P. Bennich, L. Triguero, J. Hasselström, O. Karis, L. G. M. Pettersson, and A. Nilsson, J. Chem. Phys. **112**, 1946 (2000).
[17] P. Bennich, T. Wiell, O. Karis, M. Weinelt, N. Wassdahl, A. Nilsson, M. Nyberg, L. G. M. Pettersson, J. Stöhr, and M. Samant, Phys. Rev. B **57**, 9274 (1998).
[18] J. Nordgren *et al.,* Rev. Sci. Instrum. **60**, 1690 (1989).
[19] H. Tillborg *et al.,* Phys. Rev. B **47**, 1699 (1993).
[20] J. P. Perdew and Y. Wang, Phys. Rev. B **45**, 13 244 (1992); J. P. Perdew, in *Electronic Structure of Solids,* edited by P. Ziesche and H. Eischrig (Akademie Verlag, Berlin, 1991); J. P. Perdew *et al.,* Phys. Rev. B **46**, 6671 (1992).
[21] M. E. Casida, C. Daul, A. Goursot, A. Koester, L. G. M. Pettersson, E. Proynov, A. St-Amant, and D. R. Salahub (principal authors), H. Duarte, N. Godbout, J. Guan, C. Jamorski, M. Leboeuf, V. Malkin, O. Malkina, M. Nyberg, L. Pedocchi, F. Sim, L. Triguero, and A. Vela (contributing authors), deMon-KS version 4.0, deMon Software, 1997.
[22] A. Nilsson *et al.,* Chem. Phys. Lett. **197**, 12 (1992).
[23] T. A. Albright, J. K. Burdett, and M.-H. Whenghbo, *Orbital Interactions in Chemistry* (Wiley, New York, 1985).
[24] P. S. Bagus and K. Hermann, Phys. Rev. B **33**, 2987 (1986).
[25] K. Hermann, P. S. Bagus, and C. J. Nelin, Phys. Rev. B **35**, 9467 (1987).